Association between the presence of EGFR or ALK mutations and the location of primary non-small cell lung cancer, as well as metabolic activity observed on ^{18}F-FDG PET/CT scans

INCI USLU BINER[1], TUBA INAL CENGIZ[2], ULKU YILMAZ[2], NALAN AKYUREK[3], SUNA KAVURGACI[2], PINAR AKIN KABALAK[2], DERYA KIZILGOZ[2] and EZGI GUREL AKAN[2]

[1]Department of Nuclear Medicine, Eskişehir Osmangazi University, Eskişehir 26040, Turkiye; [2]Department of Chest Diseases, Atatürk Sanatorium Training and Research Hospital, Ankara 06290, Turkiye; [3]Department of Pathology, Gazi University, Ankara 06500, Turkiye

Received October 28, 2025; Accepted June 16, 2026

DOI: 10.3892/ol.2026.15764

Abstract. The present study aimed to determine potential differences in tumor location and metabolism among patients with non-small cell lung cancer (NSCLC) and epidermal growth factor receptor (*EGFR*) mutations or anaplastic lymphoma kinase (*ALK*) rearrangements using ^{18}F-fluoro-2-deoxyglucose positron emission tomography/computed tomography (^{18}F-FDG-PET/CT). Data from ^{18}F-FDG PET/CT examinations of 112 patients with NSCLC were retrospectively reviewed. The maximum standardized uptake value (SUVmax), side (right or left), lobar localization (upper, middle or lower) and location (central or peripheral) of the lung mass were recorded. Differences in age, tumor diameter, location and SUVmax between the *EGFR*- and *ALK*-positive (+) groups were assessed. *ALK* and *EGFR* positivity were detected in 25.9% (n=29) and 74.1% (n=83) of patients, respectively. Analysis revealed comparable frequencies of *EGFR* mutations (42.2 vs. 57.8%) and *ALK* rearrangements (44.8 vs. 55.2%) in peripheral and central tumors, respectively. Of the patients with *ALK*(+), 11 (37.9%) tumors were located on the left and 18 (62.1%) on the right, whereas in *EGFR*(+) patients, 39 (47.0%) were located on the left and 44 (53.0%) on the right. *EGFR*+ and *ALK*(+) tumors were more prevalent in the upper lobe (58.6 and 60.2%, respectively). No significant association was found between the side of the main tumor, lobar position, location type and the occurrence of *ALK* rearrangements or *EGFR* mutations (P=0.530, P=0.147 and P=0.975, respectively). Mutation status was not associated with median SUVmax of the primary tumor (P=0.451), No significant difference in tumor size was observed between the groups (P=0.472) and there was no association between patient age and mutation status (P=0.422). In conclusion, tumor localization and SUVmax derived from ^{18}F-FDG PET/CT data yielded limited utility in differentiating EGFR-mutant and ALK-rearranged NSCLC. These findings should be validated in larger multicenter cohorts.

Correspondence to: Dr Inci Uslu Biner, Department of Nuclear Medicine, Eskişehir Osmangazi University, 4 Prof. Dr. Nabi Avcı Boulevard, Odunpazarı, Eskişehir 26040, Turkiye
E-mail: inciuslu@yahoo.com

Abbreviations: ALK, anaplastic lymphoma kinase; IQR, interquartile range; EGFR, epidermal growth factor receptor; NSCLC, non-small cell lung cancer; FDG-PET/CT, ^{18}F-fluoro-2-deoxyglucose positron emission tomography/computed tomography; NOS, not otherwise specified; ROI, region of interest; SUVmax, maximum standardized uptake value

Key words: EGFR, ALK, NSCLC, ^{18}F-fluoro-2-deoxyglucose positron emission tomography/computed tomography, location, maximum standardized uptake value

Introduction

Lung cancer is the leading cause of cancer-related mortality worldwide, and non-small cell lung cancer (NSCLC) accounts for ~80% of all lung cancers, with adenocarcinoma being the most frequent type (1). The identification of specific gene mutations related to the development and progression of lung cancer has led to the emergence of new treatment targets. Mutations in the epidermal growth factor receptor (*EGFR*) gene are found in 15-50% of patients with lung cancer from various ethnic backgrounds (2). Alterations in the anaplastic lymphoma kinase (*ALK*) gene occur in 3-5% of patients with NSCLC (3). The emergence of EGFR and ALK inhibitor therapies in patients with lung cancer and *EGFR* and *ALK* genomic alterations has ushered in an era of targeted therapy for advanced NSCLC, thus changing therapeutic strategies from general chemotherapy to more targeted therapies (4). The accurate identification of these driver gene mutations from small biopsy specimens for molecular analysis is of notable clinical relevance. ^{18}F-fluoro-2-deoxyglucose positron emission tomography/computed tomography (^{18}F-FDG-PET/CT) is widely used for the diagnosis and initial staging of lung cancers, and the assessment of treatment response (5). Prior studies have analyzed the association between PET/CT-derived metabolic parameters and mutation status; however, results regarding the association between *EGFR* mutations and tumor

glucose metabolism are conflicting, and to the best of our knowledge data comparing alterations in *EGFR* and *ALK* are limited. In addition to metabolic activity, prior studies have largely examined molecular subtypes; however, the possible role of anatomical constraints on these subtypes remains incompletely understood. Because *EGFR* mutations and *ALK* rearrangements are more common in specific patient subgroups, such as non-smokers and younger patients (6-8), these alterations may also be associated with different patterns of tumor anatomical localization. However, the association among tumor location, laterality and mutation status remains ambiguous. As such, the present study aimed to evaluate the association between anatomical tumor localization (lobar and central/peripheral distribution), glucose metabolism [based on maximum standardized uptake value (SUVmax)] and *EGFR*/*ALK* mutation status in patients with NSCLC. In contrast to previous studies that compared mutation-positive and wild-type tumors, the present study directly compared the anatomical and metabolic characteristics of tumors exhibiting *EGFR* mutations and *ALK* rearrangements.

Materials and methods

Study population. The present retrospective study included data from 112 patients with histopathologically confirmed NSCLC who underwent ^{18}F-FDG PET/CT-based staging between January 2013 and December 2020. The inclusion criteria were documented *EGFR* mutation and/or *ALK* translocation, PET/CT for initial staging before any systemic or local therapy and diagnostically adequate images. The exclusion criteria were absence of baseline PET/CT data, long duration between imaging and molecular analysis, previous history of malignancy and poor image quality. Most patients (97%) had adenocarcinoma histology, and those with inadequate tissue for further classification were classified as NSCLC not otherwise specified (NOS). The present study was approved by the Ankara Atatürk Sanatorium Training and Research Hospital Clinical Research Ethics Committee (approval no. 2715). Given the retrospective nature of the study, the requirement for written informed consent was waived by the ethics committee. All procedures were conducted in accordance with The Declaration of Helsinki.

PET/CT imaging process. An integrated PET/CT scanner (Biograph 6 HI-REZ; Siemens Healthineers) was used. Patients were instructed to fast ≥6 h before the examination. The procedure was performed only in patients with blood glucose levels <180 mg/dl. Each patient rested for ~45 min after intravenous administration of 0.15 mCi/kg ^{18}F-FDG. After the PET and low-dose CT scans, imaging was performed between the cranial region and the upper thigh without the use of intravenous contrast.

Interpretation of PET/CT results. FDG-PET/CT scans were reviewed by a nuclear medicine physician using an integrated workstation (Siemens Healthineers). The SUVmax was used as a quantitative measure of uptake levels on FDG-PET/CT and was defined as the maximum FDG concentration in the tumor normalized to the injected dose and patient body weight. The region of interest (ROI) was manually drawn around the pulmonary lesions to include the entire lesion within a single slice, and the maximum values within these ROIs were defined as the SUVmax. The location of the primary lung mass was then determined. Patients were divided into two groups (right and left) based on the lung side of the main mass. Tumors in the upper lobes of the right and left lungs and tumors in the middle lobe of the right lung were classified into the upper group, and lower lobe of the right and left lungs were classified into the lower group. The tumors were further classified according to their location as central or peripheral. Tumors in direct contact with the mediastinum or peribronchial location were considered to be central. PET/CT also revealed lymph nodes and distant metastases.

Testing for EGFR mutation(s) and ALK rearrangements. Pathologically confirmed samples were submitted to the Department of Pathology at Gazi University (Ankara, Turkiye) for molecular analysis.

ALK rearrangement analysis by fluorescence in situ hybridization (FISH). ALK gene rearrangements were evaluated using formalin-fixed, paraffin-embedded (FFPE) tumor tissue sections. Tissue blocks were sectioned at a thickness of 4-5 μm and mounted on positively charged glass slides. For each case, a corresponding hematoxylin and eosin-stained slide (room temperature for 15 min) was reviewed by a board-certified pathologist to delineate the areas of highest tumor density and ensure a minimum of 50-100 viable tumor cells were present for analysis.

FISH was performed using a dual-color 'break-apart' probe set (Vysis ALK Break Apart FISH Probe Kit; Abbott Pharmaceutical Co. Ltd.). The probe set consists of a 3' ALK spectrum orange/red fluorophore and a 5' ALK spectrum green fluorophore, targeting the chromosome 2p23 region. In the absence of translocation, the close proximity of these probes results in a merged yellow signal or adjacent red/green signals. The FISH procedure followed standardized laboratory protocols. Initially, slides were incubated at 60˚C 1 h to ensure tissue adherence, followed by deparaffinization in xylene and rehydration through a graded ethanol series.

Paraffin-embedded sections were incubated in an oven at 80˚C for 1 h to achieve physical deparaffinization. Subsequently, chemical deparaffinization was performed by immersing the sections in xylene for 15 min. The sections were then rehydrated by incubation in 97 and 99% ethanol for 1 min each, respectively.

Antigen retrieval was carried out in a water bath at 96˚C for 15 min using citrate buffer solution. The proteolytic treatment was performed using the Proteinase K solution supplied within the FISH kit (Abbott Pharmaceutical Co. Ltd.), which was applied to the marked area for 5 min according to the manufacturer's instructions to facilitate nuclear probe penetration

Target DNA and probes were co-denatured at 73˚C for 5 min, followed by hybridization in a humidified chamber at 37˚C for 16-24 h. Post-hybridization, stringency washes were conducted using a 0.4X SSC/0.3% NP-40 buffer at 72˚C to remove non-specifically bound probes. Nuclei were counterstained with DAPI at room temperature for 10 min.

Slides were visualized using a fluorescence microscope equipped with appropriate excitation and emission filters

(DAPI, green, orange and triple bandpass). Signal scoring was performed by two independent observers who counted a minimum of 50 non-overlapping tumor nuclei. A cell was defined as positive for ALK rearrangement if it exhibited either: Split signals, the red and green signals were separated by a distance greater than two signal diameters; or isolated single orange signals, representing the loss of the 5' green signal associated with a rearrangement. A case was interpreted as ALK-positive if >15% of the counted cells displayed these rearrangement patterns. For cases showing borderline results (10-15% positive cells), an additional 50 nuclei were evaluated by a second reader to achieve a final consensus.

EGFR mutation analysis. Molecular analysis for EGFR mutations was conducted using two specimen types: FFPE tumor tissue and/or liquid biopsy (plasma). For tissue samples, a pathologist performed a histological review to ensure a minimum tumor content of 10%, with a preference for samples >30% to optimize analytical sensitivity. For liquid biopsies, circulating cell-free DNA (cfDNA) was obtained from peripheral blood collected in specialized cell-free DNA BCT or EDTA tubes.

Genomic DNA from FFPE sections (10 μm thickness) and cfDNA from 2 ml of plasma were isolated using the cobas® DNA Sample Preparation Kit (cat. no. 05985536190; Roche Molecular Diagnostics) and the cobas cfDNA Sample Preparation Kit (cat. no. 07247737190; Roche Molecular Diagnostics), respectively. The FFPE extraction workflow included deparaffinization followed by proteinase K digestion. The plasma extraction utilized a magnetic bead-based process. All extracted DNA was quantified using fluorometric (Qubit) or spectrophotometric (NanoDrop; Thermo Fisher Scientific, Inc.) methods to ensure a minimum concentration of 2 ng/μl for tissue samples.

The cobas z 480 analyzer was employed for real-time PCR amplification and detection. The assay utilizes mutant-specific primers and fluorescently labeled TaqMan® (cobas® EGFR Mutasyon Test v2; Roche Molecular Systems, Inc.) probes to identify 42 mutations across exons 18, 19, 20 and 21 of the EGFR gene. The master mix included Uracil-N-glycosylase (AmpErase) (cobas® EGFR Mutasyon Test v2) to mitigate carry-over contamination by degrading previously amplified DNA. Thermocycling conditions were as follows: Initial denaturation was performed at 95˚C for 15 min for 1 cycle. This was followed by 42 cycles of 95˚C for 20 sec (denaturation), 53˚C for 30 sec and 72˚C for 20 sec (extension) and final extension step was carried out at 72˚C for 5 min. Targeted variants included G719X in exon 18; deletions and complex mutations in exon 19; S768I, T790M and insertions in exon 20; and L858R and L861Q in exon 21.

Automated data analysis was performed using the cobas 4800 System Software. (05200881001cobas z 480 Roche®). Each reaction included a synthetic DNA internal control to monitor for PCR inhibitors and verify extraction efficiency. The software calculated the cycle threshold for each target; results were categorized as 'mutation detected' if the fluorescent signal exceeded the predefined threshold within the validated cycle range. Run integrity was maintained through the inclusion of a positive control (containing EGFR mutant sequences) and a negative control (nuclease-free water) in every batch.

Statistical analysis. Statistical analyses were performed using SPSS software (version 21.0; IBM Corp.). The normality of data distribution was tested using the Shapiro-Wilk test. Continuous variables were expressed as mean ± standard deviation or median [interquartile range (IQR), Q1-Q3], while categorical variables were presented as frequencies and percentages. Intergroup comparisons were conducted using the independent samples t-test (for normally distributed variables) and the Mann-Whitney U test (for non-normally distributed variables). Categorical variables were compared using the χ^2 test or Fisher's exact test, as appropriate. $P<0.05$ was considered to indicate a statistically significant difference. Post hoc power analysis was performed using G*Power software (version 3.1.9.7; Heinrich-Heine-Universität Düsseldorf) (9) to assess sample size adequacy with $\alpha=0.05$, total sample size of 112, and allocation ratio of 0.35. Post-hoc power was calculated to be 0.66 for a medium-to-large effect size (Cohen's h=0.5).

Results

Data from 112 patients, diagnosed with NSCLC between January 2013 and December 2020, were included (Table I). The mean age was 59.41±12.31 years, and most patients were older than 50 years (81.3%). The median tumor size was 40 mm (IQR, 25-55). Adenocarcinoma was the most frequent histological type among the patients diagnosed in 109/112 (97%) of patients, with total of three patients diagnosed with unclassified NSCLC NOS (2.7%). A larger percentage of tumors were located in the right lung [62/112 (55.4%)]; in addition, the primary tumors were located mostly in the upper lobes (right and left) [27 (24.1%)], followed by the left lower lobe [24 (21.4%)]. The least common site was the middle lobe of the right lung [13 (11.6%)] (Fig. 1). Among all patients, *ALK* rearrangements were detected in 29 (26%) and *EGFR* mutations in 83 (74.1%). None of the patients exhibited concurrent *ALK* and *EGFR* alterations; therefore, only the ALK-positive (+) cohort was compared with the EGFR+ cohort. Representative images of ALK status evaluated by break-apart FISH are presented in Fig. 2. In ALK-negative specimens, intact loci were identified by the presence of closely linked or fused orange/green signals (Fig. 2A). Conversely, ALK rearrangement was confirmed by two distinct positive signaling patterns: The classic split pattern showing marked physical separation of the 3' (red) and 5' (green) signals (Fig. 2B), and the atypical positive pattern characterized by isolated single 3' (red) signals resulting from the deletion of the 5' probe sequence (Fig. 2C). Clinical characteristics and imaging features of the patients are summarized in Table I.

Among the patients with *ALK*+, there were 13 (44.8%) and 16 (55.2%) peripheral and central tumors, respectively, whereas for the patients with *EGFR*+, 48 (57.8%) had centrally located tumors and 35 (42.2%) had peripherally located tumors (Fig. 3). Of the patients with *ALK*+, 11 (37.9%) tumors were on the left and 18 (62.1%) on the right, whereas in those who were *EGFR*+, 39 (47.0%) were on the left and 44 (53.0%) were on the right. *EGFR* and *ALK* positivity were also more common in upper-lobe cancers (60.2 and 58.6%, respectively). There were no statistically significant associations between the side of the main tumor, lobar position, location type and occurrence of *ALK* positivity or *EGFR* mutations (P=0.530, P=0.147 and P=0.975, respectively).

Table I. Characteristics of patients and tumors (n=112).

Characteristic	Value
Age, years	59.41 (12.31)
Sex, n (%)	
Male	55 (49.1)
Female	57 (50.9)
Mutation status (%)	
ALK (+)	29 (26)
EGFR (+)	83 (74)
Primary tumor	
Tumor size, mm; median (IQR)	40 (25-55)
SUVmax; median (IQR)	12.42 (8.91-17.72)
Side of tumor, n (%)	
Right	62 (55)
Left	50 (45)
Lobar localisation, n (%)	
RUL	27 (24.1)
RML	13 (11.6)
RLL	21 (18.7)
LUL	27 (24.1)
LLL	24 (21.4)
Location, n (%)	
Central	64 (57)
Peripheral	48 (43)
Lymphadenopathy, n (%)	
Positive	102 (91)
ALK (+)	28 (97)
EGFR (+)	74 (89)
Negative	10 (9)
ALK (+)	1 (3)
EGFR (+)	9 (11)
Distant metastasis, n (%)	
Positive	64 (57)
ALK (+)	20 (69)
EGFR (+)	44 (53)
Negative	48 (43)
ALK (+)	9 (31)
EGFR (+)	39 (47)
Histology, n (%)	
Adenocarcinoma	109 (97)
NOS	3 (3)
Pleural effusion (%)	43 (38.4)

EGFR, Epidermal growth factor receptor; ALK, Anaplastic lymphoma kinase; NOS, not otherwise specified; RUL, Right upper lobe; RML, Right middle lobe; RLL, Right lower lobe; LUL, Left upper lobe; LLL, Left lower lobe; SUVmax, The maximum standardized uptake value.

All 112 primary lung cancers exhibited notably elevated FDG uptake. The median SUVmax of *ALK*+ lesions was 11.94 (IQR, 8.02-15.95), and 12.42 (IQR, 9.17-17.96) for those who were *EGFR*+; the difference between the groups was not statistically significant (P=0.451) (Fig. 4). Representative F-18 FDG PET/CT images are shown in Fig. 5.

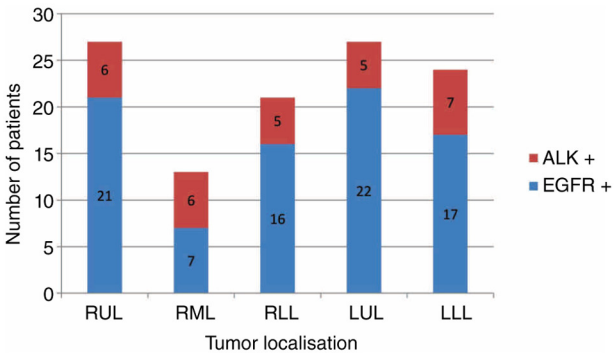

Figure 1. EGFR and ALK positivity rate in central and peripheral tumors. EGFR, epidermal growth factor receptor; ALK, anaplastic lymphoma receptor tyrosine kinase. RUL, right upper lobe), RML, right middle lobe), RLL (Right lower lobe), LUL (Left upper lobe) and LLL (Left lower lobe.

There was no significant difference in tumor size between the *ALK*+ and *EGFR*+ groups (P=0.472). The mean ages of *ALK*+ and *EGFR*+ patients were 61±13.74 and 58.86±11.80 years, respectively, with no significant association between patient age and mutation status (P=0.422). The prevalence of nodal involvement was not significantly different according to mutation status (P=0.229; Table II). The median SUVmax of lymph nodes in the cohort with *ALK* rearrangement was 6.38 (IQR, 3.42-9.71) and in the cohorts with *EGFR* mutation was 5.50 (IQR, 3.46-11.91) without a statistically significant difference (P=0.334). The clinical information, tumor localization and metabolic characteristics of the *EGFR*-positive and *ALK*-positive groups are presented in Table II. *EGFR* mutation positivity was higher among men [43/83 (55%)] and *ALK* positivity was slightly higher among women [17/29 (59%)] (Fig. 6). Distant metastasis was noted in the majority of patients with *ALK*+ [20/29 (69%)] compared with 44 (53%) with *EGFR* mutation positivity. Mutation positivity was not significantly associated with distant metastasis (P=0.135; Table II). PET/CT revealed lymph node involvement in 102 (91%) patients. FDG PET/CT identified 74 (89%) lymphadenopathies in patients with *EGFR*(+). In addition, 28/29 (97%) of patients with *ALK*+ exhibited lymph node involvement. Pleural effusions were observed in 43 patients. Specifically, pleural effusion at diagnosis was present in 13/29 (45%) patients with ALK+ and in 30/83 (36%) patients with EGFR+, with no statistically significant association between mutation status and development of effusion (P=0.408; Tables I and II).

Discussion

The present investigation aimed to compare the anatomical distribution and metabolic characteristics derived from ^{18}F-FDG PET/CT between *EGFR*-mutated and *ALK*-rearranged NSCLC. The present findings revealed that tumor side, lobar distribution, central versus peripheral localization and SUVmax were not significantly associated with mutation status, suggesting the low discriminatory power of conventional PET/CT parameters in this setting.

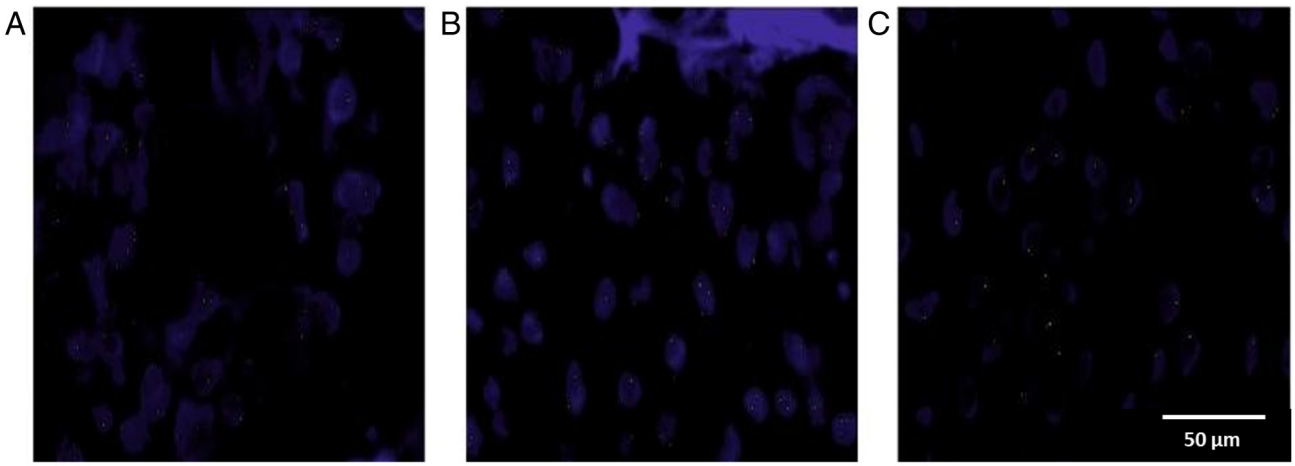

Figure 2. Representative images of ALK status evaluated by break-apart FISH (A) ALK FISH-negative specimen showing shows a signal pattern consisting of two orange/green fusion signal. (B) ALK FISH-positive specimen showing split red and green signals. (C) ALK FISH-positive specimen showing isolated single red signals. ALK, anaplastic lymphoma receptor tyrosine kinase; FISH, fluorescence in situ hybridization.

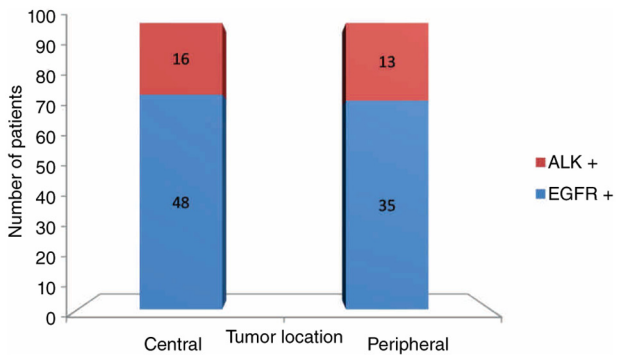

Figure 3. Distribution of EGFR-mutated and ALK-rearranged non-small cell lung cancer according to primary tumor location. EGFR, epidermal growth factor receptor; ALK, anaplastic lymphoma receptor tyrosine kinase.

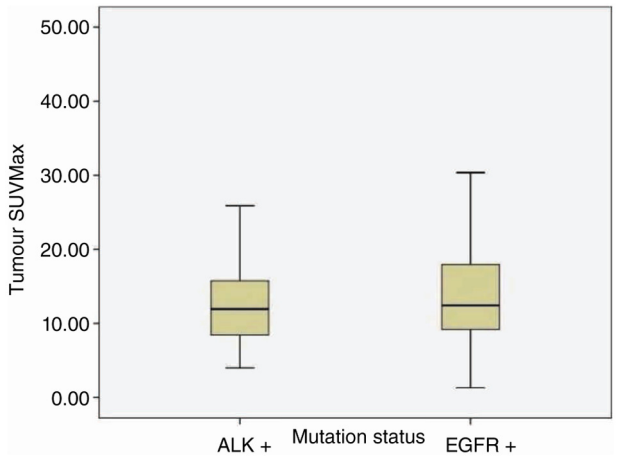

Figure 4. SUVmax value of primary tumor in EGFR and ALK positive groups. EGFR, epidermal growth factor receptor; ALK, anaplastic lymphoma receptor tyrosine kinase; SUVmax, maximum standardized uptake value.

EGFR mutations and *ALK* rearrangements are notable therapeutic targets, and non-invasive imaging biomarkers have been widely studied as adjuncts to tissue-based molecular testing. Although ^{18}F-FDG PET/CT has been proposed for mutation assessment (10), the current evidence remains controversial. Potential associations between tumor location and driver mutations have been suggested in previous studies (6,11-13); however, the present study did not observe a significant association between tumor location and mutation status.

Conflicting results have been reported in previous studies regarding the localization of tumors and molecular alterations in NSCLC. Some studies have proposed a higher incidence of central tumors in *EGFR*(+) cases (14), whereas others have not shown any significant association with *ALK* status (15). Other reports have described a higher incidence of central tumors in *ALK*+ NSCLC (16,17). These discrepancies may be explained by different patient populations, cohort sizes and the definition of tumor centrality.

Lung cancer is more often found in the upper lobes, and the present study found a greater frequency of both *EGFR*-mutant and *ALK*-rearranged tumors in this location, which is consistent with previous studies (7,18-21). While the literature indicates a relative predominance of *EGFR* mutations in the left upper lobe (22) and a more heterogeneous distribution for *ALK*-positive tumors (10,23), this upper lobe predominance did not reliably distinguish between the two molecular subtypes in the present cohort. However, differences in anatomical classification can influence the comparability between studies (24).

SUVmax, which reflects glucose metabolism in tumors, has been extensively explored as a potential imaging biomarker of genetic alterations in NSCLC; however, results have been inconclusive. Some studies have reported lower SUVmax values in *EGFR*-mutant tumors (8,25,26), whereas others have not found any significant association (27-30). Studies have identified an association between PET parameters and ALK rearrangement (4,15,31) The SUVmax did not vary significantly between the *EGFR*-mutant and *ALK*-rearranged groups in the present cohort, supporting its limited, utility for differentiating these groups. This is consistent with meta-analytic data demonstrating modest diagnostic performance of ^{18}F-FDG PET/CT for predicting *EGFR* mutation (32).

Table II. Comparison of baseline clinical, anatomical, and metabolic characteristics between EGFR-mutated and ALK-rearranged patients with non-small cell lung cancer.

Characteristic	Category	ALK(+) (n=29)	EGFR (+) (n=83)	Total (n=112)	P-value
Tumor laterality	Left	11 (37.9%)	39 (47.0%)	50 (44.6%)	0.530
	Right	18 (62.1%)	44 (53.0%)	62 (55.4%)	
Lobar distribution	Upper lobe	17 (58.6%)	50 (60.2%)	67 (59.8%)	0.147
	Middle lobe	5 (17.2%)	7 (8.4%)	12 (10.7%)	
	Lower lobe	7 (24.2%)	26 (31.4%)	33 (29.5%)	
Tumor location	Peripheral	13 (44.8%)	35 (42.2%)	48 (42.9%)	0.975
	Central	16 (55.2%)	48 (57.8%)	64 (57.1%)	
Age, years)	-	61.00±13.74	58.86±11.80	59.41±12.31	0.422
Tumor size (mm)	-	40 (27.5-55)	35 (25-55)	40 (25-55)	0.472
Distant metastasis	Positive	20 (69.0%)	44 (53.0%)	64 (57.1%)	0.135
	Negative	9 (31.0%)	39 (47.0%)	48 (42.9%)	
Lymph node involvement	Positive	28 (96.6%)	74 (89.2%)	102 (91.1%)	0.229
	Negative	1 (3.4%)	9 (10.8%)	10 (8.9%)	
Pleural effusion	Present	13 (44.8%)	30 (36.1%)	43 (38.4%)	0.408
	Absent	16 (55.2%)	53 (63.9%)	69 (61.6%)	
Primary tumor SUVmax	-	11.94 (8.02-15.95)	12.42 (9.17-17.96)	12.42 (8.91-17.72)	0.451
Lymph node SUVmax	-	6.38 (3.42-9.71)	5.50 (3.46-11.91)	5.62 (3.45-11.52)	0.334

Data are presented as n (%), mean ± standard deviation or median (Q1-Q3). Pearson χ^2 or Fisher's exact test was used for categorical variables, while independent samples t-test (bootstrap method) or Mann-Whitney U test (Monte Carlo simulation) was used for continuous variables, as appropriate. No patients with concurrent ALK rearrangement and EGFR mutation were identified. ALK, anaplastic lymphoma kinase; EGFR, epidermal growth factor receptor; SUVmax, maximum standardized uptake value.

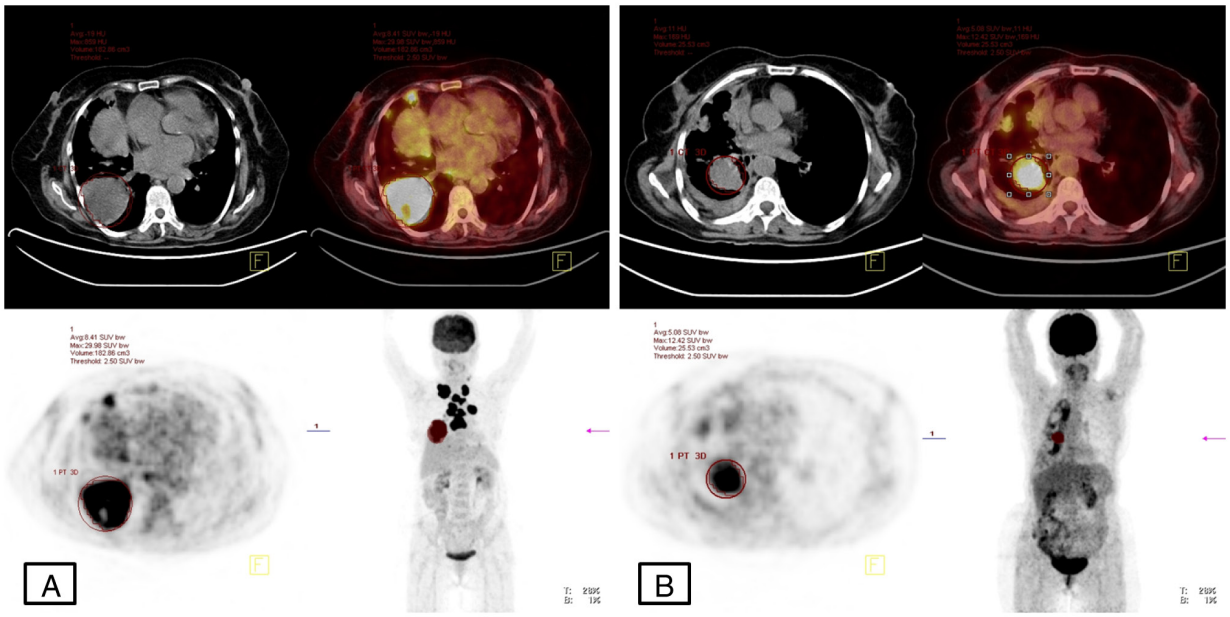

Figure 5. Representative F-18 FDG PET/CT images of patients with non-small cell lung cancer. (A) *EGFR*-positive case demonstrating primary tumor FDG uptake (B) *ALK*-positive case demonstrating primary tumor FDG uptake. FDG-PET/CT, ^{18}F-fluoro-2-deoxyglucose positron emission tomography/computed tomography.

The absence of an association between tumor location and mutation status indicates that the distribution of tumor location is primarily determined by structural and environmental factors (such as bronchial anatomy and carcinogen exposure) (26), rather than by oncogenic changes. Similarly, the absence of metabolic differences indicates that FDG uptake is associated with complex tumor biology rather than mutation-specific effects. The EGFR and ALK signaling pathways activate downstream cascades, such as PI3K/AKT and MAPK, and tumor metabolism is modulated

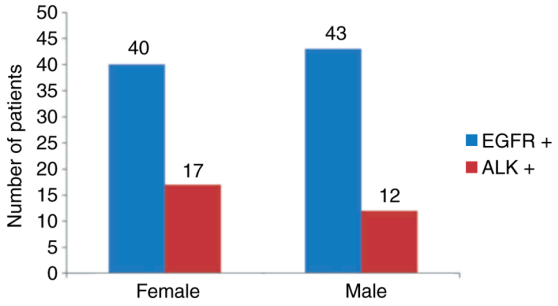

Figure 6. Relationship between *EGFR* and *ALK* mutation status and sex. EGFR, epidermal growth factor receptor; ALK, anaplastic lymphoma receptor tyrosine kinase.

by intratumoral heterogeneity, hypoxia and the tumor microenvironment (33-36), thus limiting the utility of SUVmax as a surrogate biomarker.

The clinical importance of these findings lies in the complementary role of ^{18}F-FDG PET/CT in the initial diagnostic workup. SUVmax and tumor location were not independent predictors of *EGFR* or *ALK* status; however, the metabolic profile may be an additional aspect of the overall assessment of tumor behavior. Specifically, *ALK*-rearranged tumors are more often associated with advanced metastatic disease, consistent with their known aggressive phenotype (8,31). PET/CT can be helpful in assessing the extent of disease when tissue sampling is limited; however, it should not be used in place of molecular testing.

Recent studies have demonstrated the potential of combining PET/CT parameters, clinical parameters, and radiomic or deep learning-based features to improve the molecular characterization of NSCLC (37-41). Imaging must be considered within the framework of multimodal diagnosis, in which treatment selection must be based on molecular testing as the gold standard. In previous studies, mutation status has been associated with clinicopathological factors such as age, sex and tumor size (42-45). In the present cohort, these associations were not significant, which may be due to the limited sample size and heterogeneity of the population.

The present study has several limitations. First, its retrospective, single-center design, relatively small sample size and imbalance between the *EGFR* and *ALK* subgroups may limit the generalizability of the findings. In addition, metabolic assessment was limited to SUVmax, and no advanced PET-derived parameters such as metabolic tumor volume or total lesion glycolysis were included. Differences in anatomical classification, such as the right middle lobe being grouped within the upper lobes, may also have influenced the comparisons. A post hoc power analysis demonstrated 66% statistical power, indicating that smaller associations may not have been detected. Internal validation strategies such as resampling or subgroup analyses were not performed because of the limited subgroup size. Another notable limitation is the lack of direct mechanistic validation. Although potential biological pathways linking EGFR and ALK signaling to tumor metabolism were discussed, these interpretations remain speculative because integrated molecular or functional analyses were not available. Therefore, the findings should be interpreted as exploratory and hypothesis-generating.

In conclusion, tumor localization and SUVmax derived from ^{18}F-FDG PET/CT data yielded limited utility in differentiating *EGFR*-mutant and *ALK*-rearranged NSCLC. These findings should be interpreted in the context of the study limitations and validated in larger multicenter cohorts. Future studies including advanced metabolic and radiomic approaches may improve non-invasive molecular characterization and support more precise personalized management of patients diagnosed with NSCLC.

Acknowledgements

The authors would like to thank Professor Cengiz Bal (Department of Biostatistics, Medicine Faculty, Osmangazi University, Eskişehir, Turkiye) for his support to the statistical analysis. The present manuscript was presented as a poster presentation at the 36th National Nuclear Medicine Congress, Cyprus (May 08-12, 2024).

Funding

No funding was received.

Availability of data and materials

The data generated in the present study may be requested from the corresponding author.

Authors' contributions

IUB, UY, TIC and NA contributed to the conception and design of the study. SK, PAK, DK and EGA were responsible for data collection and literature search. IUB analyzed the images, interpreted the results and wrote the initial draft of the manuscript. UY, TIC and NA supervised the study and revised the manuscript. IUB and TIC confirm the authenticity of all the raw data. All authors read and approved the final version of the manuscript.

Ethics approval and consent to participate

The Ethics Committee of Atatürk Sanatorium Training and Research Hospital approved the study with approval no. 2715, and the study was conducted in accordance with the principles set forth in The Declaration of Helsinki.

Patient consent for publication

Not applicable.

Competing interests

The authors declare that they have no competing interests.

References

1. Budak E and Yanarates A: The role of PET/CT in determining EGFR mutation and ALK rearrangement in patients with lung adenocarcinoma. Ann Med Res 27: 634, 2020.
2. Byers TE, Vena JE and Rzepka TF: Predilection of lung cancer for the upper lobes: An epidemiologic inquiry. J Natl Cancer Inst 72: 1271-1275, 1984.

3. Cho A, Hur J, Moon YW, Hong SR, Suh GJR, Kim YJ, Im DJ, Hong YJ, Lee HJ, Kim YJ, *et al*: Correlation between EGFR gene mutation, cytologic tumor markers, ^{18}F-FDG uptake in non-small cell lung cancer. BMC Cancer 16: 224, 2016.
4. Choi H, Paeng JC, Kim DW, Lee HK, Parkı CM, Kang KW, Chung HK and Lee DS: Metabolic and metastatic characteristics of ALK-rearranged lung adenocarcinoma on FDG PET/CT. Lung Cancer 79: 242-247, 2013.
5. Cruz CSD, Tanoue LT and Matthay RA: Lung cancer: Epidemiology, etiology, and Prevention. Clin Chest Med 32: 605-644, 2011.
6. Gupta R, Amanam I, Rahmanuddin S, Mambetsariev I, Wang Y, Huang H, Reckamp K, Vora L and Salgia R: Anaplastic lymphoma kinase (ALK)-positive tumors. Am J Clin Oncol 42: 337-344, 2019.
7. Midha A, Dearden S and McCormack R: EGFR mutation incidence in non-small-cell lung cancer of adenocarcinoma histology a systematic review and global map by ethnicity (mutMapII). Am J Cancer Res 5: 2892-2911, 2015.
8. Mori M, Hayashi H, Fukuda M, Honda S, Kitazaki T, Shigematsu K, Matsuyama N, Otsubo M, Nagayasu T, Hashisako M, *et al*: Clinical and computed tomography characteristics of non-small cell lung cancer with ALK gene rearrangement: Comparison with EGFR mutation and ALK/EGFR-negative lung cancer. Thorac Cancer 10: 872-879, 2019.
9. Faul F., Erdfelder E, Lang AG and Buchner A: G*Power 3: A flexible statistical power analysis program for the social, behavioral, and biomedical sciences. Behav Res Methods 39: 175-191, 2007.
10. Lv Z, Fan J, Xu J, Wu F, Huang Q, Guo M, Liao T, Liu S, Lan X, Liao S, *et al*: Value of ^{18}F-FDG PET/CT for predicting EGFR mutations and positive ALK expression in patients with non-small cell lung cancer: A retrospective analysis of 849 Chinese patients. Eur J Nucl Med Mol Imaging 45: 735-750, 2017.
11. Du B, Wang S, Cui Y, Liu G, Li X and Li Y: Can ^{18}F-FDG PET/CT predict EGFR status in patients with non-small cell lung cancer? A systematic review and meta-analysis. BMJ Open. 11: e044313, 2021.
12. Förster GJ, Misch D, Kollmeier J, Köcer T, Griff S, Kaiser D and Bauer TT: Der SUV im FDG-PET als prädiktiver Wert einer EGFR-Mutation beim nicht-kleinzelligen Lungenkarzinom. Pneumologie 66: 201, 2012.
13. Hsu JS, Huang MS, Chen CY, Liu GC, Liu TC, Chong IW, Chou SH and Yang CJ: Correlation between EGFR mutation status and computed tomography features in patients with advanced pulmonary adenocarcinoma. J Thorac Imaging 29: 357-363, 2014.
14. Huang CT, Yen RF, Cheng MF, Hsu YC, Wei PF, Tsai YJ, Tsai MF, Shih YJ, Yang CH and Yang PC: Correlation of F-18 fluorodeoxyglucose-positron emission tomography maximal standardized uptake value and EGFR mutations in advanced lung adenocarcinoma. Med Oncol 27: 9-15, 2009.
15. Igde MH, Ozturk A, Oruç O, Öztaş S and Kavas M: The relationship of PET/CT SUVmax with EGFR mutation status and ALK rearrangement in lung adenocarcinoma. Hell J Nucl Med 25: 188-119, 2022.
16. Ito M, Yamashita Y, Miyata Y, Ohara M, Tsutani Y, Ikeda T, Misumi K, Harada H and Omori K: Prognostic impact of the primary tumor location based on the hilar structures in non-small cell lung cancer with mediastinal lymph node metastasis. Lung Cancer 76: 93-97, 2012.
17. Jeong JC, Lee HY, Han J, Jeong JY, Lee KS, Choi YL and Choi YJ: Role of imaging biomarkers in predicting anaplastic lymphoma kinase-positive lung adenocarcinoma. Clin Nucl Med 40: e34-e39, 2015.
18. Kinsey CM, Estepar RSJ, Zhao Y, Yu X, Diao N, Soygunu RS, Wain JC, Mark EJ, Washko G and Christiani DC: Invasive adenocarcinoma of the lung is associated with the upper lung regions. Lung Cancer 84: 145-150, 2014.
19. Lee YW, Park YS, Park S and Lee CH: Poor prognosis of NSCLC located in lower lobe is partly mediated by lower frequency of EGFR mutations. Sci Rep 10: 14933, 2020.
20. Mendoza DP, Lin JJ, Rooney MM, Chen T, Sequist LV, Shaw AT and Digumarthy SR: Imaging features and metastatic patterns of advanced ALK-rearranged non-small cell lung cancer. Am J Roentgenol 214: 766-774, 2019.
21. Miyauchi E, Motoi N, Ono H, Ninomiya H, Ohyanagi F, Nishio M, Okumura S, Ichinose M and Ishikawa Y: Distinct characteristics of small cell lung cancer correlate with central or peripheral origin. Medicine 94: e2324, 2015.
22. Lee SM, Bae SK, Jung SJ and Kim JK: FDG uptake in non-small cell lung cancer is not an independent predictor of EGFR or KRAS mutation status. Clin Nucl Med 40: 950-958, 2015.
23. Mak RH, Digumarthy SR, Muzikansky A, Engelman JA, Shepard JO, Choi NC and Sequist LV: Role of ^{18}F-Fluorodeoxyglucose positron emission tomography in predicting epidermal growth factor receptor mutations in non-small cell lung cancer. Oncologist 16: 319-326, 2011.
24. Lee HW, Lee CH and Park YS: Location of stage I-III non-small cell lung cancer and survival rate: Systematic review and meta-analysis. Thorac Cancer 9: 1614-1622, 2018.
25. Na II, Byun BH, Kim KM, Cheon GJ, Choe DH, Koh JS, Lee DY, Ryoo BY, Baek H, Lim SM, *et al*: ^{18}F-FDG uptake and EGFR mutations in patients with non-small cell lung cancer: A single-institution retrospective analysis. Lung Cancer. 67: 76-80, 2009.
26. Nilssen Y, Brustugun OT, Fjellbirkeland L, Helland A, Møller B, Wahl SGF and Solberg S: Distribution and characteristics of malignant tumours by lung lobe. BMC Pulm Med 24: 106, 2024.
27. Park HS, Harder EM, Mancini BR and Decker RH: Central versus peripheral tumor location: influence on survival, local control, and toxicity following stereotactic body radiotherapy for primary non-small-cell lung cancer. J Thorac Oncol 10: 832-837, 2015.
28. Putora PM, Szentesi K, Glatzer M, Rodriguez R, Müller J, Baty F and Früh M: SUVmax and Tumour Location in PET-CT Predict Oncogene Status in Lung Cancer. Oncol Res Treat 39: 681-686, 2016.
29. Rizzo S, Petrella F, Buscarino V, Maria FD and Raimondi S: CT radiogenomic characterization of EGFR, K-RAS, and ALK mutations in non-small cell lung cancer. Eur Radiol 26: 32-42, 2015.
30. Rosell R, Carcereny E, Gervais R, Vergnenegre A, Massuti B, Felip E, Palmero R, Garcia-Gomez R, Pallares C, Sanchez JM, *et al*: Spanish Lung Cancer Group in collaboration with Groupe Français de Pneumo-Cancérologie and Associazione Italiana Oncologia Toracica Erlotinib versus standard chemotherapy as first-line treatment for European patients with advanced EGFR mutation-positive non-small-cell lung cancer (EURTAC): A multicentre, open-label, randomised phase 3 trial. Lancet Oncol 13: 239-246, 2012.
31. Lv Z, Fan J, Xu J, Wu F, Huang Q, Guo M, Liao T, Liu S, Lan X and Liao S: Value of ^{18}F-FDG PET/CT for predicting EGFR mutations and positive ALK expression in patients with non-small cell lung cancer: A retrospective analysis of 849 Chinese patients. Eur J Nucl Med Mol Imaging 45: 735-750, 2017.
32. Sun W, Yang X, Liu Y, Yuan Y and Lin D: Primary tumor location is a useful predictor for lymph node metastasis and prognosis in lung adenocarcinoma. Clin Lung Cancer 18: e49-e55, 2017.
33. Deng H, Chen Y, Li P, Hang Q, Zhang P, Jin Y and Chen M: PI3K/AKT/mTOR pathway, hypoxia, and glucose metabolism: Potential targets to overcome radioresistance in small cell lung cancer. Cancer Pathog Ther 27: 56-66, 2022.
34. Makinoshima H, Takita M, Saruwatari K, Umemura S, Obata Y, Ishii G, Matsumoto S, Sugiyama E, Ochiai A, Abe R, *et al*: Signaling through the Phosphatidylinositol 3-Kinase (PI3K)/Mammalian Target of Rapamycin (mTOR) axis is responsible for aerobic glycolysis mediated by glucose transporter in epidermal growth factor receptor (EGFR)-mutated lung adenocarcinoma. J Biol Chem 290: 17495-17504, 2015.
35. Semenza GL: HIF-1: Upstream and downstream of cancer metabolism. Curr Opin Genet Dev 20: 51-56, 2010.
36. Skoulidis F and Heymach JV: Co-occurring genomic alterations in non-small-cell lung cancer biology and therapy. Nat Rev Cancer 19: 495-509, 2019.
37. Ouyang W, Zhu C, Li Y, Huang H, Li F and Ling L: Assessing the neurotoxic risks of triethyl citrate in daily environmental exposure using network toxicology and molecular docking. Ecotoxicol Environ Saf 297: 118225, 2025.
38. Chen H, Jiang T, Yang Y, Cai G, Jiang Y and Ouyang W: Exploring the carcinogenic potential of bisphenol A in lung adenocarcinoma: Molecular mechanisms, key gene insights, and immune microenvironment impacts. Front Immunol 16: 1647807, 2025.
39. Ouyang W, Peng Q, Lai Z, Huang H, Huang Z, Xie X, Lin R, Wang Z, Yao H and Yu Y: Synergistic role of activated CD4+ memory T cells and CXCL13 in augmenting cancer immunotherapy efficacy. Heliyon 10: e27151, 2024

40. Yu Y, Ouyang W, Huang Y, Huang H, Wang Z, Jia X, Huang Z, Lin R, Zhu Y, Yalikun Y, *et al*: Artificial intelligence-based multi-modal multi-tasks analysis reveals tumor molecular heterogeneity, predicts preoperative lymph node metastasis and prognosis in papillary thyroid carcinoma: a retrospective study. Int J Surg 111: 839-856, 2025.
41. Ouyang W, Deng Z, Li Y, Chi W, Huang Z, Zhan C, Li M, Wang D, Li F, Liu Y and Ling L: Traditional Chinese medicine in cerebral infarction: Integrative strategies and future directions. Phytomedicine 143: 156841, 2025.
42. Tseng CH, Chen KC, Hsu KH, Tseng JS, Ho CC, Hsia TC, Su KY, Wu MF, Chiu KL and Liu CM: EGFR mutation and lobar location of lung adenocarcinoma. Carcinogenesis 37: 157-162, 2016.
43. Vallee A, Sagan C, Loupp AGL, Bach K, Dejoie T and Denis MG: Detection of EGFR gene mutations in non-small cell lung cancer: Lessons from a single-institution routine analysis of 1,403 tumor samples. Int J Oncol 43: 1045-1051, 2013.
44. Yamamoto S, Korn RL, Oklu R, Migdal C, Gotway MB, Weiss GJ, Iafrate AJ, Kim DW and Kuo MD: ALK Molecular phenotype in Non-Small cell lung cancer: CT radiogenomic characterization. Radiology 272: 568-576, 2014.
45. Yang B, Wang QG, Lu M, Ge Y, Zheng YJ, Zhu H and Lu G: Correlations Study between ^{18}F-FDG PET/CT metabolic parameters predicting epidermal growth factor receptor mutation status and prognosis in lung adenocarcinoma. Front Oncol 18: 589, 2019.